Climate Dynamics manuscript No.
(will be inserted by the editor)

The Influence of Global Sea Surface Temperature Variability on the Large-Scale Land Surface Temperature

Nicholas L. Tyrrell · Dietmar Dommenget · Claudia Frauen · Scott Wales · Mike Rezny

Received: date / Accepted: date

Abstract In global warming scenarios, global land surface temperatures (T_{land}) warm with greater amplitude than sea surface temperatures (SSTs), leading to a land/sea warming contrast even in equilibrium. Similarly, interannual variability shows increased co-variability of T_{land} with SSTs leading to a land/sea contrast in natural variability. This work investigates the land/sea contrast in natural variability based on global observations, coupled general circulation model simulations and idealised atmospheric general circulation model simulations with different SST forcings.

The land/sea temperature contrast in interannual variability is found to exist in observations and models to a varying extent in global, tropical and extra-tropical bands. There is agreement between models and observations in the tropics but not the extra-tropics. Causality in the land-sea relationship is explored with modelling experiments forced with prescribed SSTs, where an amplification of the imposed SST variability is seen over land. The amplification of T_{land} to tropical SST anomalies is due to the enhanced upper level atmospheric warming that corresponds with tropical moist convection over oceans leading to upper level temperature variations that are larger in amplitude than the source SST anomalies. This mechanism is similar to that proposed for explaining the equilibrium global warming land/sea warming contrast.

The link of the T_{land} to the dominant mode of tropical and global interannual climate variability, the El Niño Southern Oscillation (ENSO), is found to be an indirect and delayed connection. ENSO SST variability affects the oceans outside

N. L. Tyrrell, D. Dommenget, C. Frauen
ARC Centre of Excellence for Climate System Science
School of Mathematical Sciences, Monash University, Clayton, Victoria, Australia
E-mail: nicholas.tyrrell@monash.edu

S. Wales
ARC Centre of Excellence for Climate System Science
School of Earth Sciences, The University of Melbourne, Australia

Mike Rezny
Met Office, Exeter, EX1 3PB, United Kingdom

the tropical Pacific, which in turn leads to a further, amplified and delayed response of T_{land}.

Keywords Land sea thermal contrast · interannual variability · Tropical troposphere · ENSO · Pacemaker experiment · Atmospheric Bridge

1 Introduction

In a transient climate the global land surface temperatures (T_{land}) warm with greater amplitude than sea surface temperatures (SSTs), leading to a land/sea warming contrast. The ratio of land to sea warming tends to a value of around 1.5 (Sutton et al 2007, Lambert and Chiang 2007, Compo and Sardeshmukh 2008, Dommenget 2009). Previous studies have shown the land/sea warming contrast is not simply due to the larger heat capacity of the ocean when compared to land, but is a result of the dynamics of the climate system. Sutton et al (2007) described an energy balance argument; assuming the anomalous downward surface energy flux is equal over land and ocean the land/sea warming contrast is caused by the difference in the partitioning of the upward energy flux into sensible and latent heat. Lambert and Chiang (2007) proposed that the stability of land/sea contrast over annual, 5 year and longer timescales is maintained by a land to ocean heat flux where the ability of the ocean to absorb the extra heat leads to a damping of T_{land} variability. In this scenario the value of the land/sea contrast depends on the ratio of the land and sea climate sensitivity parameters, and can be related to the results of Sutton et al (2007). However, as stated by Byrne and OGorman (2013) the energy balance argument does not give a sufficient quantitative value of land warming. Joshi and Gregory (2008) proposed a conceptual model to explain how the SSTs can force T_{land}, leading to a land/sea warming contrast above unity. There is a level in the atmosphere above which there is no significant land/sea contrast and thermal anomalies are transported efficiently around the globe. The lapse rate below that level is affected by temperature and moisture and different land and ocean lapse rates cause the land temperatures to reach an equilibrium warmer than the oceans.

Dommenget (2009) demonstrates the ability of oceans to cause a land/sea contrast on interannual and longer time scales, arguing that the asymmetric forcing of ocean to land is not only due to the asymmetry in area but also due to atmospheric water vapour feedbacks. Thus the land/sea warming contrast is a natural phenomena that also applies to internal interannual to decadal climate variability. When we think of the land/sea contrast in natural variability we can recognise a number of differences relative to that seen in global warming: Firstly, global warming is mostly a coherent warming on global scale with a time evolution that is only going upwards. Furthermore in natural climate variability we have inhomogeneous warming and cooling patterns, some of them are regional others are more global, some of them have coherent warming and cooling (e.g. multi-pole structures) at the same time, some of them are closer to the land and some are over tropical warm ocean regions and others are over the colder extra-tropical oceans. When we analyse the land/sea contrast in natural climate variability we have to take these structures into account.

When looking at the interannual variability of land and ocean the El Niño-Southern Oscillation and its teleconnections are the leading source of variability on a global scale. Klein, Soden, and Lau (1999) discuss the concept of an atmospheric bridge as a method of communicating temperature anomalies from the equatorial Pacific to the remote tropical oceans (outside the Pacific). Similarly, Chiang and Sobel (2002) discuss a mechanism for warming of remote tropical oceans during El Niño conditions. The tropical tropospheric temperature (T_{tropos}) increases during El Niño, and is largely uniform across the tropical strip, 20S-20N. They attributed the amplified response over land to the smaller thermal inertia and reduced cooling due to evaporation. Chiang and Lintner (2005) further found an almost instantaneous response of T_{land} to El Niño and an ocean response with a 2-3 month lag. The ratio between T_{tropos} and the surface warming signal was 1:1 for land but only 1:0.3 for oceans. Their findings support the mechanism over oceans described by Chiang and Sobel (2002) as holding true on the larger scale they were investigating. No mechanism was proposed for land warming, the higher ratio of warming was attributed to differing heat capacities of ocean and land. The processes of the atmospheric bridge responsible for the El Niño teleconnections are similar in nature to the processes of the land/sea contrast as discussed in Joshi and Gregory (2008), suggesting that the same principles are active.

The study presented here discusses the large-scale land/sea contrast in natural variability, focusing on interannual timescales. We will analyse the characteristics of the large-scale land/sea contrast variability in observations and Couple General Circulation Models (CGCMs) from the CMIP5 data base. The role of the SST in forcing the land variability will be analysed in Atmospheric General Circulation Models (AGCMs) forced with observed SSTs and in a series of sensitivity experiments with an AGCM coupled to a slab ocean model or with fixed SST boundary conditions forced with different idealised SST forcings. Our analysis will discuss the differences between tropical and extra-tropical regions.

In this article, the data and model simulations are described in the section 2. Section 3 will discuss the evidence for the land/sea contrast larger than unity in natural variability in observations and model simulations. This analysis will also explore some of the regional differences in the ocean to land connection. Section 4 dicsusses a series of sensitivity experiments that explore the role of the SST forcing, the differences between tropical and extra-tropical regions and that highlight the role on El Niño forcing. Section 5 is an analysis of the mechanisms involved, illustrating how the SST forcing is amplified over land to result into a land/sea contrast larger than unity. In the final section the study will be closed with a summary and discussion.

2 Data and Methods

The observational surface temperature datasets used were the Climatic Research Unit Temperature data set, version 4 (CRUTEM4) (Brohan et al 2006) for T_{land} and the Hadley Centre SST data set, version 2 (HadSST2) (Rayner et al 2006)for the SST, T_{ocean}. Temperature data previous to 1950 was excluded in the analysis of the land/sea interactions as the smaller data coverage area can cause errors in the statistical comparison of the two datasets (Dommenget 2009).

For the analysis of CGCMs we used all available pre-industrial control runs from the CMIP5 datasets (Taylor et al 2012), see Table 1. The sensitivity experiments were performed with the UK Meteorological Office Unified Model AGCM with HadGEM2 atmospheric physics (Davies et al (2005); Martin et al (2010); Martin et al (2011)) at an atmospheric resolution of N48 ($3.75^\circ \times 2.5^\circ$). This was coupled to prescribed SSTs or a slab ocean. The slab ocean assumes a constant mixed layer depth of 50 metres and is forced by flux correction terms to have on average the HadISST1 1950–2010 SST climatology (Wang et al Submitted).

Three primary types of experiments were conducted: AMIP-type; sensitivity to mean SST increases; and El Niño pattern forcing experiments, see Table 2. The latter being similar to a 'pacemaker' experiment, as described by Alexander 1992a, Alexander 1992b, Lau and Nath 2000 and Lu et al 2011. The AMIP type runs used HadISST1 from 1870 to 2010. Simulations forced with idealised SST patterns used a 12 month climatology of the HadISST1 data from 1950-2010 as the reference control climate. The division between tropics and extra-tropics for these experiments was chosen to be 28°N/S, with the tropical forcing applied to the oceans in the zonal band bordered by 28°N/S, and the extra-tropical forcing applied from 28°N/S to the poles. For the model resolution used this most closely divides the oceans in half by area, with slightly more area in the extra-tropics. For the El Niño pattern forcing experiments a canonical El Niño pattern was generated using HadISST1 data and a linear regression between NINO3 and SSTs, shown in Figure 1. This pattern was imposed in the tropical Pacific between 30^oN/S and 155^oE to the eastern boundary of the Pacific. The values of the anomaly was based on the regression values, with a maximum temperature anomaly of 1.41K. It was oscillated with a period of 4 years, peaking in January. Outside of the tropical Pacific there were two scenarios; fixed SSTs using the HadISST1 1950-2010 climatology, and the slab ocean.

All further analysis is based on annual mean anomalies with one exception in Section 4.2, which is based on monthly mean anomalies for monthly mean lag-lead correlations. The land/sea contrast, $R_{L/S}$, is defined by the following regression model;

$$T_{land} = R_{L/S} \cdot T_{ocean} \tag{1}$$

where

$$R_{L/S} = \rho_{land,ocean} \cdot \frac{\sigma_{land}}{\sigma_{ocean}} \tag{2}$$

With T_{land} and T_{ocean} as the annual mean surface temperature anomalies of land and ice-free oceans, respectively, $\rho_{land,ocean}$ is the correlation coefficient between T_{land} and T_{ocean}, and $\sigma_{land}, \sigma_{ocean}$ are the standard deviations of T_{land}, T_{ocean}.

3 Evidence of land/ocean temperature contrast in observations and models

In this first analysis section we will characterise $R_{L/S}$ in natural internal climate variability in observations and model simulations. The focus here will be to illustrate that $R_{L/S} > 1.0$ exists on interannual time scales in observations and models, but has some significant regional differences.

We start the analysis with a look at the observations and the CMIP5 CGCM simulations. We then focus on AMIP-type simulations, in which the SST is given as the forcing and the T_{land} are responding, which allows us to draw some conclusions about the potential of the SST variability as the driving mechanism of T_{land} variability.

3.1 Observations

The land/sea relation of interannual surface temperature variability for different regions is shown in Figure 2 and Table 3. Firstly, we can note that in the comparison of the time series of the global mean T_{land} and the global mean T_{ocean} they both have some common interannual fluctuations (correlation of 0.6; statistically significant at the 99% level), indicating that the global land and ocean have co-variability on the interannual time-scales. The correlation indicates that about 1/3 of the total variance of T_{land} in the global mean is co-variable with T_{ocean} and the majority, 2/3, of the total variance of T_{land} is independent of T_{ocean}, assuming a simple linear relation. We can further note that the variability over land is much larger than over oceans. The ratio of the standard deviations is 2.5. The combination of the correlation and the ratio in standard deviations leads to the global mean $R_{L/S} = 1.43$. Thus the variability in surface temperature that is co-variant between the land and the oceans is about 43% larger in amplitude over land than over oceans.

In the next step we look at different zonal bands. We split the globe into a tropical band (30^oN/S round the equator) and two extra-tropical bands (polewards of 30^oN/S round the equator), with the combined area of the latter two bands having the same area as the tropical band. First of all it is interesting to note that in all three zonal bands $R_{L/S}$ is smaller than in the global mean. This suggests that $R_{L/S}$ on the global scale is more dominant than on regional scales. In the tropical regions (Fig.2b) the correlation between T_{land} and T_{ocean} is much stronger than for the global means, and although $R_{L/S} = 1.2$ is larger than unity, it is still smaller than the global value. Thus the variability in surface temperature that is co-variant between the land and the oceans is about 20% larger over land than it is over oceans. The larger correlation also indicates that about 2/3 of the total variance of T_{land} in the tropics is co-variable with T_{ocean}, again assuming a simple linear relation. To some extent these differences in the land/sea contrast relative to the global mean may reflect the different land and ocean fractions in the tropics. The relatively small land fraction suggets that land points are on average closer to ocean points and would thus be more strongly linked to the nearby SST variability. However, the differences in the land/sea contrast may also reflect differences in physical interactions between land and oceans, which will be addressed in the further analysis below.

In the extra-tropical regions of the Northern Hemisphere the land/sea contrast is about unity and therefore weaker than in the tropics, but the correlation between T_{land} and T_{ocean} is about as large as for the global mean. The extra-tropical regions of the Northern Hemisphere are marked by a pronounced low-frequency evolution, that is about the same amplitude in both T_{land} and T_{ocean}. However, some interannual fluctuations appear to be similar in T_{land} and T_{ocean} as well (e.g. around the years 1965 and 1990), but with much larger amplitudes over land. In the extra-tropical regions of the Southern Hemisphere the land/sea contrast is weaker than in the other zonal bands. Again, this may to some extent be related to the distribution of the land fraction and in particular to the isolated location of the main southern hemispheric land mass of Antarctica.

Since land and ocean areas are unequally distributed over the zonal bands, the correlations between the zonal bands may be of interest. In particular, most of the interannual SST variability is in the tropical oceans, so one may wonder if T_{land} of the extra-tropical regions of the Northern Hemisphere is more strongly related to the tropical or global T_{ocean} rather than to the extra-tropical Northern Hemisphere T_{ocean}. Table 4 shows a number of interesting correlations between the zonal bands and between land and ocean areas. First of all we can note that the global mean T_{ocean} is strongly dominated by the tropical T_{ocean}, which is clearly related to the dominant mode of variability —ENSO— and to the fact that the tropical oceans are the largest part of the global oceans. We can further note that the extra-tropical regions of the Northern Hemisphere oceans have a moderate positive correlation to the global mean, but not to the tropical T_{ocean}. The global and Northern Hemisphere T_{land} are nearly identical, as most of the land is in the Northern Hemisphere. Although global T_{ocean} is dominated by the tropical T_{ocean} the global and the Northern Hemisphere T_{land} have only a moderate correlation to tropical T_{ocean}, suggesting only a weak direct influence of the tropical T_{ocean} on Northern Hemisphere T_{land}.

In summary, in the observations we find a land/sea contrast in the temperature variability that has, in most regions, stronger amplitudes over land than over oceans. In particular in the tropics there is a strong link between T_{land} and T_{ocean} variability, whereas in the extra-tropical regions of the Northern Hemisphere the link appears to be much weaker.

3.2 Coupled General Circulation Model Simulations (CMIP5)

We now explore how CGCM simulations can represent the land/sea contrast in natural variability. This helps us to understand the mechanisms behind the land/sea contrast as well as providing a much larger data base, which allows us to explore the characteristics of the land/sea contrast in more detail. We therefore analysise the preindustrial (no external forcings) simulations from the CMIP5 data base, using the multi model ensemble of 35 models.

In analog to the analysis of the observations (e.g. Fig. 1 and Table 3) we summarise the statistics of the land/sea contrast from all models for the global, tropical and the two extra-tropical hemispheres in Table 3 and 4. The CMIP5 simulations multi model mean shows a very similar land/sea contrast in both $R_{L/S}$ and the correlation value for both global and tropical means. They also have a very weak connection between Southern Hemispheric extra-tropical land and ocean. However, in the Northern Hemisphere extra-tropics the models show a weaker link between ocean and land variability than observations. The CMIP5 models also do not show much impact from the Northern Hemispheric T_{ocean} to global mean T_{ocean}. In a similar way the Northern Hemispheric T_{land} does not dominate global mean T_{land} in the CMIP5 simulation as it does in observations.

We can now look at the inter-model variations. The scatter plots in Figure 3 show that amongst the CMIP5 models the land/sea correlation in the tropics is linearly related to the global value of the land/sea correlation (Fig. 2b). Models with a strong land/sea connection in the tropics also tend to have a stronger global land/sea connection (Fig. 2 a). The extra-tropical interactions are not strongly related to the global values. We can further note that the spread in the extra-tropical values in both $R_{L/S}$ and the correlation values are much larger than in the tropics. This suggests that the CMIP5 models disagree much more on the extra-tropical land/ocean interactions than they do in the tropics.

The results suggest that tropical values of the land/sea correlation are more important in determining the global value, and tropical processes connecting ocean and land surface temperatures on these timescales are unrelated to the extra-tropics. Again it should be noted here that global T_{land} is dominated by the large land fractions in the extra-tropical Northern Hemisphere. The tropical land fraction is much smaller. In turn, T_{ocean} is dominated by the large tropical SST variability. Thus, the strong link between global and tropical land/sea correlation suggests that it is the tropical SST variability that is a significant cause of the land/sea contrast.

The relationship between global mean T_{land} and the regional SST variability is explored next to illustrate which patterns of variability are related to land variability. We correlate T_{land} with local SST variability, see Figure 4. Here the timeseries of T_{land} and surface temperature anomalies of all CMIP5 models were combined and the annually averaged global T_{land} is correlated with surface temperatures. The same analysis was done in Dommenget [2009] (Fig. 3a) for observations. The CMIP5 model results are largely similar to the observations as shown in Dommenget [2009], but due to the much larger database the emerging pattern is much less noisy and more details can be seen.

The CMIP5 models show a strong relationship between global T_{land} and tropical ocean and land temperatures. All the tropical land masses are highly correlated and there are distinct patterns of high correlations in the tropical oceans. There are some similarities in the patterns between the ocean basins; there is a minimum at the equator and on the eastern edge of each of the basins. Larger correlations in all three tropical ocean basins are on the western side of the basin. The highest correlations are in the Indian ocean where there is a large region with correlation values above 0.6. The patterns seem to suggest that the SST variability close to the land regions and in the upwind direction of the prevailing easterly trade winds are most strongly linked to the global T_{land}. It is remarkable in this figure that the most dominant pattern of SST variability, El Niño, is not directly visible here, as there is a local minimum of correlations on the equator.

In the extra-tropical regions we see bands of negative correlations in both hemispheres. Thus positive anomalies in the global mean T_{land} are related to negative SST anomalies over large parts of the extra-tropical oceans. This SST pattern is somewhat similar to the ENSO teleconnections or decadal variations of global SST variability (Lau and Nath 1996 & Dommenget and Latif 2008). It indicates that changes in the extra-tropical atmospheric circulation linked to the tropical SST variability can lead to the negative SST correlations in the extra-tropical regions.

To summarise, coupled global climate models are effective in simulating the land/sea contrast in natural variability. Tropical values of the land/sea correlation and ratio of standard deviations are consistent between models and observations. The largest discrepancy between observations and models is in the extra-tropics, especially the Northern Hemisphere. These results indicate that the physical processes controlling these metrics are well represented by the models in the tropics but may not be as well simulated in the extra-tropics.

3.3 Atmospheric response to SST forcing (AMIP-simulations)

In the previous section we have characterised the land/sea contrast in observations and CGCM simulations. We now address the causality of this link by assuming that the land is responding to SST variability. Thus testing the idea that the natural SST variability is leading to an amplified response over land. We therefore do a series of AMIP-type experiments, in which we prescribe historical SST variability globally or in parts of the global oceans and analyse the response of the T_{land} and other atmospheric variables.

Figure 5 shows the same plots as Figure 2 except for an AMIP simulation using the an AGCM forced with the historical global HadISST1 SST variability (see data section for details). The land/sea contrast values are largely consistent with observations. The globally averaged values are higher than observed; there is a lower ratio of standard deviation between land and oceans but a higher correlation. The AMIP tropically averaged values of land/sea contrast, correlation and ratio of standard deviations are almost identical to observations. AMIP runs are forced only by SSTs, so the high correlation between land and ocean surface temperatures in the tropics indicates a direct, strong connection from ocean to land. For both the tropical and global mean the values of land/sea contrast are larger than unity, indicating that the SST forcing is amplified over the continents.

The extra-tropical Northern Hemisphere land/sea contrast value is substantially lower than observed. The low values of land/sea contrast in the extra-tropics are due to the low correlations between ocean and land; there is still a much greater variance of land compared to ocean temperatures. The low correlation of annual mean temperature implies that on these timescales the influence of the extra-tropical oceans is either less significant or more subtle and less direct than in the tropics. If we assume that the models capture the correct ocean-land interactions and that the observed extra-tropical land/sea contrast is accurate, then we have to conclude that the extra-tropical land/sea contrast is not forced by the SST variability. It may be the atmospheric internal variability forcing the extra-tropical SST variability and T_{land}, with the T_{land} having the larger amplitudes. This picture is consistent with Barsugli and Battisti (1998).

In Figure 6 f-tests are used to measure the increase in annual temperature variability due to SST variability at the surface and at the 300hPa pressure level relative to a simulation with fixed SST climatology. Figure 6 a) and b) show that global SST variability has a substantial impact on the tropical atmospheric and surface temperature variability. However, in the extra-tropical regions the impact is much weaker, but still statistically significant in some regions.

In order to separate the influence of the tropical SST variability from that of the extra-tropical SST, we repeat the AMIP experiment forced with the historical SST variability just in the tropics or just in the extra-tropical regions. The impact of the tropical SST variability is similar to the global SST variability, with a clear and strong impact in the tropical regions. The AMIP simulation with just the extra-tropical SST variability has only a very weak to no impact on the regional (grid-box scale) atmospheric and surface temperature variability. However, if we compare the global AMIP versus the tropical only AMIP run we still can see a somewhat larger increase in variance over land in the global AMIP run. This indirectly suggests that the extra-tropical SST forcing does play a role, although it is much smaller than the tropical forcing. In summary the AMIP experiments suggest a clear tropical SST forcing to the atmospheric and land surface temperatures, but a much weaker or no forcing from the extra-tropical SST.

4 Sensitivity experiments

In the previous section we illustrated that the SST variability is forcing an amplified response in the T_{land} variability. It was also shown that the link to tropical SSTs was much stronger than the link to extra-tropical SSTs. This result suggests that the atmosphere and land are more sensitive to tropical SST variability, but it may also illustrate that tropical SST variability is stronger than extra-tropical or may have patterns of variability that affect the land more strongly than those from the extra-tropics. In the first set of sensitivity experiments we explore the differences between tropical and extra-tropical SST forcing and in the second set of sensitivity experiments we take a closer look at ENSO SST variability, which is the main driver of global SST variability.

4.1 SST perturbation experiments

In order to address the sensitivity of the atmosphere and land to identical SST anomalies from the tropical or extra-tropical regions we conduct a series of idealised sensitivity experiments, with homogeneous increases in the SST by +1K. These experiments are similar to some of the classical SST response experiments done in previous studies in the context of global warming or climate sensitivity (Cess et al 1990, Dommenget 2009, Compo and Sardeshmukh 2008).

Figure 7 shows the surface temperature response (control removed) from the +1K experiments; where +1K was added to the oceans in the tropics, extra-tropics or globally. In response to a tropical SST perturbation there is a large tropical response, greatest over equatorial South America and Africa, India and the maritime continent (Fig.7 a). The tropical +1K ocean perturbation leads to $T_{land} > +1$K in most tropical areas. Thus the SST forcing is amplified. The extra-tropical land the response to the tropical forcing is not significant everywhere, but some regions also show an amplified response to the tropical SST forcing (e.g. central Asia and parts of Europe and North America). An extra-tropical T_{land} response to tropical SST is seen for seasonal averages in the winter months of each hemisphere, the Northen Hemsiphere winter response is shown in Figure 7e.

When looking at the annual mean response of T_{land} to extra-tropical SST perturbations there is little significant response, however for seasonal averages both hemispheres show a significant response in their respective winter months, shown for the Northern Hemisphere in Figure 7 e-g. The response of T_{land} is also amplified in some regions relative to the initial perturbation. However, the extra-tropical forcing again leads to a weaker land response than the tropical forcing, as was also found in the AMIP simulations. Also similar to the AMIP simulations we again find that the global SST forcing has a bigger impact than the tropical only forcing for the annual mean. In addition the response of the global SST forcing is greater than the superposition of the tropical and extra-tropical forcing (comparing Fig.7 c and d). This again indirectly suggests that the extra-tropical SST forcing does lead to a significant land response.

4.2 Influence of ENSO

On inter-annual timescales ENSO is the most significant global climate driver. It is therefore remarkable that in the analysis of the CMIP5 model simulations the NINO3 region did not show up with a high correlation to global T_{land} (see Fig.4). The ENSO region in the tropical Pacific has a lower correlation with T_{land} than adjacent regions and the other ocean basins. Using the combined monthly mean CMIP5 surface temperature anomalies, Fig.8 e) shows the lagged correlations between NINO3 SST and global T_{land}. The NINO3 region is seen to lead global land by 4 months. Typically land has a fast response time to forcings, which would not result in a 4 month delay, so this result suggests that the full land response is not directly forced by the NINO3 SST but is most likely caused by something else. This other forcing may be delayed to the ENSO variability by about 4 months. Since we have seen in Fig.4 that global T_{land} is highly correlated to other tropical ocean SST, it seems likely that T_{land} is linked to the slower ocean response in the remote tropical oceans and not directly to the NINO3 region.

To address this question we conducted a series of idealised ENSO-response experiments. In the first experiment we prescribe an oscillating ENSO pattern (a regression between NINO3 and SSTs shown in Fig.1) in the tropical Pacific and fixed SST climatologies elsewhere. The oscillation period of the ENSO signal is 4 years, peaking in January. In the second experiment we allow SST variability outside the tropical Pacific simulated by a simple slab ocean model. Thus, in the second experiment the global ocean SSTs can respond to the oscillating ENSO pattern forcing.

Figure 8 (i-l) shows cross-correlations from the ENSO-FIXSST and ENSO-Slab forcing experiments. In i) and j) we see that for the fixed SST experiment the global and tropical land responds to the ENSO-like forcing (red line), and does so without the delay seen in Figure 8 e). When a slab ocean is introduced the land responds with a realistic delay of around 4 months. The peak slab ocean response is at 6 months, implying that the land is responding immediately to the initial Pacific ocean forcing and then subsequently to the delayed slab ocean response. The delayed land response is also associated with a higher correlation to the NINO3 region. Comparing the global and tropical averages, the main difference is the magnitude of the peak correlation, but in the tropics the slab ocean also results in the peak land correlation being higher than the peak ocean correlation. So the delayed response of the remote tropical oceans to a Pacific ocean forcing explains both the delayed land response and some part of the amplification of the oceanic temperature signal over land. In the extra-tropics there is only a very weak influence of the ENSO forcing on land temperatures in the sensitivity experiments (Fig. 8 g, h), and the tropical Pacific has little influence on the slab ocean in the extra-tropics. The observations and CMIP5 models also don't show a significant relationship between the extra-tropics and NINO3.

5 Mechanism for the continental amplification of the SST forcing

$R_{L/S}$ larger than unity in the SST forced experiments indicates that the land's response to SST variability is amplified. We now wish to explore how this amplification is physically realised. We therefore compare the simulation without any SST variability (FIXSST) with the simulation with the oscillating ENSO signal in the tropical Pacific and the slab ocean SST variability in the rest of the oceans (ENSO-Slab).

We first take a look at the vertical structure of the relationship between land and ocean temperatures to highlight the link between oceans and land in the free troposphere. Using tropical averages above land and ocean points, Figure 9 shows regression values for the T_{tropos} at different pressure levels as a function of the surface temperature T_{land} and T_{ocean}. In the simulation without any SST variability the higher level tropical temperatures over land areas are only weakly related to T_{land}, indicating that the atmospheric internal (independent of SST variability) T_{land} variability is limited to the near surface layers and is not strongly related to the upper free T_{tropos} (green dashed line in Fig. 9 a). In the simulation with SST variability the upper level temperature shows a strong relationship with the surface T_{land} variability (solid green line in Fig. 9 a). In particular the relation of T_{land} with upper level temperatures over ocean areas shows a strong increase with height, with values larger than unity between 500hPa to 200hPa (solid blue line in Fig. 9 a).

Over ocean regions we see a clear increase in the relationship between the surface T_{ocean} and the 500hPa to 200hPa level temperature variability (blue line in Fig. 9 b). This is a well known signature of moisture convection; for a unity warming at the surface the upper level temperatures will warm more, due to the latent heat release by moist convection (Joshi et al (2007), Byrne and O'Gorman (2013), Dommenget (2009), etc.). This signature appears to be transported to the land regions, which leads to the similarity in the regressions between T_{land} and T_{ocean} with upper level T_{tropos} over ocean regions (compare solid blue lines in Fig. 9 a and b).

The combination of the regression values suggests the following scenario for the land amplification of the SST forcing: SST variability in the tropical ocean regions leads to T_{tropos} at higher levels above the oceans with larger amplitudes due to the latent heat release by moist convection. The well mixed free troposphere transports the amplified SST signal over land. Here the surface T_{land} feels the increased upper level T_{tropos} and follows the upper temperature variability, but with smaller amplitudes. Thus the amplification of the SST variability is not happening over land, but is achieved locally over ocean regions by moist convection.

We now take a look at the regional differences in this upper level T_{tropos} amplification. We split the land areas into subregions allowing us to focus on large-scale T_{land} values and average out the smaller scale T_{land} variability to get a clearer picture of the large-scale interactions, for example Africa was divided into southern, central and northern regions and the variables were averaged over each of these areas. The areas are roughly selected by similar sizes and by averaging over regions with similar mean climates in humidity and temperature. Figure 10(a-c) shows linear regression coefficients between area average T_{land} and upper level (500-100hPa) T_{tropos} above. We will first of all focus on the tropical regions and then discuss the extra-tropical regions.

As in the previous analysis (Fig. 9) the regressions for the FIXSST run dont show any strong connections between surface temperature and T_{tropos}. In some regions the values are even negative. Compare this to the regressions for the ENSO-Slab forced run where strong positive regressions exist between the surface and the troposphere in the tropics (Fig. 10 b). To highlight the influence of the SST variability we plot the difference in the regression values (Fig. 10 c). It shows that tropical ocean forcing leads to a large increase in tropospheric forcing of land surface temperatures across all the tropics.

A look at a few other atmospheric variables helps us to better understand the ocean forcing of the land areas. The regressions between downward longwave radiation (LW) and T_{land} mostly fit to the relationship between T_{tropos} and T_{land} with increases in T_{tropos} alongside with increases in LW. However, the increase in LW (Fig 10 f) is larger than one would expect from the pure black body radiation effect of the T_{tropos} increase (Fig. 10 c) with a emissivity lower than unity. According to the black body radiation effect, the LW increase should be about $1W/m^2/K$, but it is significantly larger than that over Africa and South America. This suggests that the increase in LW is not only due to the T_{tropos} increase.

The short wave radiation (SW) and indirectly the total cloud cover (in reversed sign) shows a significant reduction over most of the tropical regions. This suggests that SW counteracts the land warming and would thus be a negative feedback. However, the thermal radiation effect related to the increases in cloud cover would further increase the LW response, which partly explains the large LW effect. The surface humidity is also increasing in most tropical regions with T_{land}, which is mostly the opposite of what we see in the control FIXSST atmospheric internal variability (Fig. 10 j). This would further strengthen the LW effect by increasing the emissivity of the tropospheric layers.

The response in sea level pressure (SLP) is a good first order indicator of atmospheric circulation response. In the control FIXSST atmospheric internal variability SLP is mostly negative for positive T_{land} (negative regression values in Fig. 10 m). However, in the oscillating ENSO signal simulation SLP is positive for large regions. This is a reflection of the atmospheric circulation changes during El Niño. This is particularly strong over the Maritime Continent and Australia. The strong SLP response over Australia to some extent explains why we do not see a strong response in T_{tropos} and LW over Australia.

In the extra-tropical regions there is much less of an effect visible from the SST variability. Here it has to be noted that the oscillating ENSO simulation also demonstrates SST variability in the extra-tropical regions as simulated by the slab ocean that is in its amplitude about as large as observed. This has also been demonstrated in other studies (Alexander 1992a, Alexander 1992b, Dommenget and Latif 2002). However, no substantial influence from the T_{tropos}, LW or humidity can be found. SW and therefore total cloud cover do show some impact, which may be related to circulation changes, as SLP responses in the extra-tropical regions are also more pronounced which suggests that atmospheric circulation responses in these regions are important.

6 Summary and discussion

The aim of this study was to analyse the large-scale land/sea warming and cooling contrasts in natural variability in observations and model simulations. Comparing the statistics between observations, coupled climate model simulations and idealised atmosphere-only SST forced simulations, we found some consistent characteristics of the land/sea contrast, estimated the role of the SST in forcing the land and described the main tropical forcing and amplification mechanism for the tropical SST to influence T_{land}.

The observations, CGCM simulations from the CMIP5 models and AMIP-type forced AGCM experiments show a quite consistent picture for the tropical and global land/sea interaction. $R_{L/S}$ is larger than unity on both a tropical and a global scale. The global $R_{L/S}$ tends to be larger than any zonal band, suggesting that the land/sea warming and cooling contrast in natural variability is stronger on the larger-scale. However, substantial regional differences exist in this. In particular, in the extra-tropical regions the $R_{L/S}$ tends to be smaller or insignificant. We also find some disagreement in the Northern hemisphere extra-tropics with the observations showing a significant land/sea correlation that doesn't exist in the CGCM simulation. However, it is unclear from the analysis whether this points towards a model problem or an observational data problem.

An important part of this study was determining causality in the land/sea relationship. This was investigated with AMIP runs and sensitivity experiments. Forcing an AGCM model with observed SSTs results in a realistic land/sea contrast in the tropics, while in the Northern Hemisphere extra-tropics the value differed from observations but was still similar to coupled models. This can indicate that: either the observed covariance between land and ocean is not SST forced and comes from internal atmospheric variability or a land to ocean feedback exists, which clearly will be missing from AMIP runs. Assuming the observed strong $R_{L/S}$ in the Northern Hemisphere extra-tropics is real the lag of a strong $R_{L/S}$ in the CMIP CGCM simulations either suggests that the correct atmosphere-ocean interaction is missing or indicates that the CGCM simulations do not produce the right kind of natural SST variability. The latter may indeed be a problem, as it has been shown that the simulated modes of SST variability in the extra-tropical oceans in the CMIP5 CGCM simulations are indeed quite different from the observed (Wang et al Submitted).

An interesting aspect of the tropical connection to T_{land} is the relatively small correlation with the NINO3 SST index and the role of the remote tropical oceans in the response of T_{land}. The slow response of the Indian and Atlantic tropical basins to the Pacific ocean forcing leads to the delay of the T_{land} response to the NINO3 SST index by several months (Lau and Nath 1996, Chiang and Lintner 2005, Su et al 2005). In addition to the delay, the combined Pacific/remote ocean forcing further amplifies the T_{land} response. With the help of the idealised ENSO-like experiments we confirmed that the delayed land response is due to the slowly responding remote tropical oceans and this leads to increased variability of T_{land}. The process of how T_{land} is being forced by ENSO can be outlined as follows: the NINO3 SST anomalies in the tropical Pacific are transported via the troposphere and land responds without delay, the remote tropical oceans respond on a timescale of 4–6 months, and tropical land also responds quickly to this delayed forcing which leads to a peak in the land's response to ENSO at a delay of 3 months.

The large sensitivity (amplification) of T_{land} to tropical ocean temperature anomalies is due to the enhanced upper level atmospheric warming that goes along with tropical SST variability. The latent heat released by moist convection leads to upper level temperature variations that are larger in amplitude than the source SST anomalies. The amplified positive and negative anomalies are transported to land, leading to an increase in temperature variability over land compared to oceans. This mechanism is essentially the same as that proposed for explaining the equilibrium global warming land/sea warming contrast (e.g. Joshi and Gregory (2008), Dommenget (2009) or Byrne and O'Gorman (2013)). The link via the upper level amplification by moist convection suggests that the climate will be more sensitive to SST variability in warm ocean regions that allow for increases in deep convections. The processes we explained don't extend to the extra-tropics due to the lack of strong large-scale moist convection, and as such we don't fully explain extra-tropical values of the land/sea contrast. However the Northern Hemispheric correlation values seen in observations, and the non-linear model response of the extra-tropical continents to tropical and extra-tropical ocean forcings indicate that the land/sea connection outside of the tropics is more subtle but still important.

Table 1 CMIP5 models used in this study. 100 years of the piControl run was used from each model.

Originating Group(s)	Country	Model
CSIRO and BOM	Australia	ACCESS1.0
Beijing Climate Center, China Meteorological Administration	China	BCC-CSM1.1
Beijing Climate Center, China Meteorological Administration	China	BCC-CSM1.1-m
GCESS, Beijing National University	China	BNU-ESM
National Center for Atmospheric Research	USA	CCSM4
National Center for Atmospheric Research	USA	CESM1-BGC
National Center for Atmospheric Research	USA	CESM1-CAM5
National Center for Atmospheric Research	USA	CESM1-FASTCHEM
National Center for Atmospheric Research	USA	CESM1-WACCM
Centro Euro-Mediterraneo per i Cambiamenti	Italy	CMCC-CM
Centro Euro-Mediterraneo per i Cambiamenti	Italy	CMCC-CMS
CSIRO and QCCCE	Australia	CSIRO-Mk3-6-0
Meteo-France/Centre National de Recherches Meteorologiques	France	CNRM-CM5
Canadian Centre for Climate Modelling and Analysis	Canada	CanESM2
Institute of Atmospheric Physics and Chinese Academy of Sciences	China	FGOALS-g2
Institute of Atmospheric Physics and Chinese Academy of Sciences	China	FGOALS-s2
The First Institution of Oceanography	China	FIO-ESM
Geophysical Fluid Dynamics Laboratory	USA	GFDL-CM3
Geophysical Fluid Dynamics Laboratory	USA	GFDL-ESM2G
Geophysical Fluid Dynamics Laboratory	USA	GFDL-ESM2M
NASA / Goddard Institute for Space Studies	USA	GISS-E2-H
NASA / Goddard Institute for Space Studies	USA	GISS-E2-R
Hadley Centre for Climate Prediction and Research/Met Office	UK	HadCM3
Hadley Centre for Climate Prediction and Research/Met Office	UK	HadGEM2-CC
Hadley Centre for Climate Prediction and Research/Met Office	UK	HadGEM2-ES
Institute for Numerical Mathematics	Russia	INM-CM4
Institut Pierre Simon Laplace	France	IPSL-CM5A-LR
Institut Pierre Simon Laplace	France	IPSL-CM5A-MR
Institut Pierre Simon Laplace	France	IPSL-CM5B-LR
Atmosphere and Ocean Research Institute (AORI), National Institute for Environmental Studies (NIES) and Japan Agency for Marine-Earth Science and Technology (JAMSTEC)	Japan	MIROC5
AORI, NIES and JAMSTEC	Japan	MIROC-ESM
Max Planck Institute for Meteorology	Germany	MPI-ESM-LR
Max Planck Institute for Meteorology	Germany	MPI-ESM-P
Max Planck Institute for Meteorology	Germany	MPI-ESM-MR
Meteorological Research Institute	Japan	MRI-CGCM3
Norwegian Climate Centre	Norway	NorESM1-M
Norwegian Climate Centre	Norway	NorESM1-ME

Table 2 Idealised model simulations discussed in this study. Atmospheric component was HadGEM2 at N48 resolution.

Name	*Ocean*	*Time*	*Notes*
AMIP-global	HadISST1	1870-2012	
AMIP-tropics	Tropics: HadISST1 Extra-tropics: FIXSST	1870-2012	Climatological SSTs with anomalies applied in tropics
AMIP-extra-tropics	Extra-tropics: HadISST1 Tropics: FIXSST	1870-2012	Climatological SSTs with anomalies applied in extra-tropics
FIXSST	Climatology	100 years	Climatological SSTs based on HadISST1 1950-2013
+1K Global	FIXSST, +1K	100 years	Climatology with +1K added to global oceans
+1K Tropics	FIXSST, +1K in Tropics	100 years	Climatology with +1K added to tropical oceans
+1K Extra-tropics	FIXSST +1K in Extra-tropics	100 years	Climatology with +1K added to extra-tropical oceans
Slab	50m mixed layer ocean	100 years	
ENSO-FIXSST	FIXSST, El Niño pattern	100 years	Climatology with oscillating pattern in tropical Pacific
ENSO-slab	Slab, El Niño pattern	100 years	50m mixed layer ocean with oscillating pattern in tropical Pacific

Table 3 Annual mean T_{land} and T_{ocean} used to calculate land/sea contrast, ratio of land/sea standard deviations and correlation coefficient between land and sea. Observations is HadSST2 and CruTEMP4 data. CMIP5 is combined pre-industrial control runs from 35 models, showing one standard deviation between the individual models. AMIP run was forced with HadISST1. ENSO-like run forced with oscillating canonical ENSO pattern in the tropical Pacific, slab ocean elsewhere.

Data set and region	L/S contrast	L/S correlation	Ratio Std Dev
Observations			
Global	1.43	0.58	2.45
Tropical	1.19	0.81	1.48
NH Extra-tropics	1.00	0.61	1.64
SH Extra-tropics	0.22	0.10	2.28
CMIP5, multi-model mean values			
Global	1.26 ± 0.23	0.64 ± 0.13	1.97 ± 0.26
Tropics	1.35 ± 0.16	0.87 ± 0.06	1.55 ± 0.15
NH extra-tropics	0.32 ± 0.30	0.19 ± 0.18	1.63 ± 0.29
SH extra-tropics	0.03 ± 0.68	0.01 ± 0.20	3.41 ± 0.70
AMIP run			
Global	1.27	0.74	1.72
Tropical	1.26	0.88	1.43
NH Extra-tropics	0.53	0.34	1.59
SH Extra-tropics	0.64	0.16	2.41
ENSO-Slab			
Global	1.50	0.71	2.13
Tropical	1.17	0.85	1.37
NH Extra-tropics	0.57	0.28	2.08
SH Extra-tropics	-0.42	-0.11	3.69

Table 4 Correlation coefficient of annual mean T_{land} and T_{ocean} between regions

Region	Observations	CMIP5	AMIP
Global Ocean - Tropical Ocean	0.81	0.92	0.90
Global Ocean - N Hemis ExTr. Ocean	0.37	0.09	0.36
Tropical Ocean - N Hemis ExTr. Ocean	0.15	-0.16	0.02
Tropical Ocean- Tropical Land	0.81	0.87	0.88
Tropical Ocean- Global Land	0.40	0.66	0.78
Gobal Land - N Hemis. ExTr. Land	0.95	0.74	0.78

Acknowledgements We would like to thank Tobias Bayr, Michael Byrne and Penny McQueen for useful discussions and comments. This study was supported by the ARC Centre of Excellence in Climate System Science (CE110001028) and the ARC project 'Beyond the linear dynamics of the El Nino Southern Oscillation' (DP120101442). The model simulations were computed on the National Computational Infrastructure in Canberra.

References

Alexander MA (1992a) Midlatitude AtmosphereOcean Interaction during El Niño. Part I: The North Pacific Ocean. Journal of Climate 5(9):944–958, DOI 10.1175/1520-0442(1992)005¡0944:MAIDEN¿2.0.CO;2, URL http://journals.ametsoc.org.ezproxy.lib.monash.edu.au/doi/abs/10.1175/1520-0442(1992)005¡0944:MAIDEN¿2.0.CO;2

Alexander MA (1992b) Midlatitude AtmosphereOcean Interaction during El Niño. Part II: The Northern Hemisphere Atmosphere. Journal of Climate 5(9):959–972, DOI 10.1175/1520-0442(1992)005¡0959:MAIDEN¿2.0.CO;2, URL http://journals.ametsoc.org.ezproxy.lib.monash.edu.au/doi/abs/10.1175/1520-0442(1992)005¡0959:MAIDEN¿2.0.CO;2

Barsugli JJ, Battisti DS (1998) The Basic Effects of AtmosphereOcean Thermal Coupling on Midlatitude Variability*. Journal of the Atmospheric Sciences 55(4):477–493, DOI 10.1175/1520-0469(1998)055¡0477:TBEOAO¿2.0.CO;2, URL http://journals.ametsoc.org.ezproxy.lib.monash.edu.au/doi/abs/10.1175/1520-0469(1998)055%3C0477%3ATBEOAO%3E2.0.CO%3B2

Brohan P, Kennedy JJ, Harris I, Tett SFB, Jones PD (2006) Uncertainty estimates in regional and global observed temperature changes: A new data set from 1850. Journal of Geophysical Research 111(D12):D12,106, DOI 10.1029/2005JD006548, URL http://doi.wiley.com/10.1029/2005JD006548

Byrne MP, O'Gorman PA (2013) Link between landocean warming contrast and surface relative humidities in simulations with coupled climate models. Geophysical Research Letters DOI 10.1002/grl.50971, URL http://onlinelibrary.wiley.com/doi/10.1002/grl.50971/abstract

Byrne MP, OGorman PA (2013) LandOcean Warming Contrast over a Wide Range of Climates: Convective Quasi-Equilibrium Theory and Idealized Simulations. Journal of Climate 26(12):4000–4016, DOI 10.1175/JCLI-D-12-00262.1, URL http://journals.ametsoc.org.ezproxy.lib.monash.edu.au/doi/abs/10.1175/JCLI-D-12-00262.1

Cess RD, Potter GL, Blanchet JP, Boer GJ, Del Genio AD, Déqué M, Dymnikov V, Galin V, Gates WL, Ghan SJ, Kiehl JT, Lacis AA, Le Treut H, Li ZX, Liang XZ, McAvaney BJ, Meleshko VP, Mitchell JFB, Morcrette JJ, Randall DA, Rikus L, Roeckner E, Royer JF, Schlese U, Sheinin DA, Slingo A, Sokolov AP, Taylor KE, Washington WM, Wetherald RT, Yagai I, Zhang MH (1990) Intercomparison and interpretation of climate feedback processes in 19 atmospheric general circulation models. Journal of Geophysical Research 95(D10):16,601, DOI 10.1029/JD095iD10p16601, URL http://doi.wiley.com/10.1029/JD095iD10p16601

Chiang J, Lintner B (2005) Mechanisms of remote tropical surface warming during El Nino. Journal of climate 18(1999):4130–4149, URL http://journals.ametsoc.org/doi/pdf/10.1175/JCLI3529.1

Chiang JCH, Sobel AH (2002) Tropical Tropospheric Temperature Variations Caused by ENSO and Their Influence on the Remote Tropical Climate*. Journal of Climate 15(18):2616–2631, DOI 10.1175/1520-0442(2002)015¡2616:TTTVCB¿2.0.CO;2, URL http://dx.doi.org/10.1175/1520-0442(2002)015¡2616:TTTVCB¿2.0.CO 2 http://journals.ametsoc.org/doi/abs/10.1175/1520-0442(2002)015¡2616:TTTVCB¿2.0.CO;2

Compo GP, Sardeshmukh PD (2008) Oceanic influences on recent continental warming. Climate Dynamics 32(2-3):333–342, DOI 10.1007/s00382-008-0448-9, URL http://www.springerlink.com/index/10.1007/s00382-008-0448-9

Davies T, Cullen MJP, Malcolm AJ, Mawson MH, Staniforth A, White AA, Wood N (2005) A new dynamical core for the Met Office's global and regional modelling of the atmosphere. Quarterly Journal of the Royal Meteorological Society 131(608):1759–1782, DOI 10.1256/qj.04.101, URL http://doi.wiley.com/10.1256/qj.04.101

Dommenget D (2009) The Oceans Role in Continental Climate Variability and Change. Journal of Climate 22(18):4939–4952, DOI 10.1175/2009JCLI2778.1, URL http://journals.ametsoc.org/doi/abs/10.1175/2009JCLI2778.1

Dommenget D, Latif M (2002) Analysis of observed and simulated SST spectra in the midlatitudes. Climate Dynamics 19(3-4):277–288, DOI 10.1007/s00382-002-0229-9, URL http://link.springer.com/10.1007/s00382-002-0229-9

Dommenget D, Latif M (2008) Generation of hyper climate modes. Geophysical Research Letters 35(2):L02,706, DOI 10.1029/2007GL031087, URL http://doi.wiley.com/10.1029/2007GL031087

Joshi M, Gregory J (2008) Dependence of the land-sea contrast in surface climate response on the nature of the forcing. Geophysical Research Letters 35(24):1–6, DOI 10.1029/2008GL036234, URL http://www.agu.org/pubs/crossref/2008/2008GL036234.shtml

Joshi MM, Gregory JM, Webb MJ, Sexton DMH, Johns TC (2007) Mechanisms for the land/sea warming contrast exhibited by simulations of climate change. Climate Dynamics 30(5):455–465, DOI 10.1007/s00382-007-0306-1, URL http://www.springerlink.com/index/10.1007/s00382-007-0306-1

Klein S, Soden B, Lau N (1999) Remote sea surface temperature variations during ENSO: Evidence for a tropical atmospheric bridge. Journal of Climate 12:917–932, URL http://journals.ametsoc.org/doi/full/10.1175/1520-0442(1999)012%3C0917:RSSTVD%3E2.0.CO%3B2

Lambert FH, Chiang JCH (2007) Control of land-ocean temperature contrast by ocean heat uptake. Geophysical Research Letters 34(13):1–5, DOI 10.1029/2007GL029755, URL http://www.agu.org/pubs/crossref/2007/2007GL029755.shtml

Lau NC, Nath MJ (1996) The Role of the Atmospheric Bridge in Linking Tropical Pacific ENSO Events to Extratropical SST Anomalies. Journal of Climate 9(9):2036–2057, DOI 10.1175/1520-0442(1996)009¡2036:TROTBI¿2.0.CO;2, URL http://dx.doi.org/10.1175/1520-0442(1996)009¡2036:TROTBI¿2.0.CO 2 http://journals.ametsoc.org/doi/abs/10.1175/1520-0442(1996)009¡2036:TROTBI¿2.0.CO;2

Lau NC, Nath MJ (2000) Impact of ENSO on the Variability of the AsianAustralian Monsoons as Simulated in GCM Experiments. Journal of Climate 13(24):4287–4309, DOI 10.1175/1520-0442(2000)013¡4287:IOEOTV¿2.0.CO;2, URL http://journals.ametsoc.org.ezproxy.lib.monash.edu.au/doi/abs/10.1175/1520-0442(2000)013¡4287:IOEOTV¿2.0.CO;2

Lu J, Zhang M, Cash B, Li S (2011) Oceanic forcing for the East Asian precipitation in pacemaker AGCM experiments. Geophysical Research Letters 38(12):n/a–n/a, DOI 10.1029/2011GL047614, URL http://doi.wiley.com/10.1029/2011GL047614

Martin GM, Milton SF, Senior CA, Brooks ME, Ineson S, Reichler T, Kim J (2010) Analysis and Reduction of Systematic Errors through a Seamless Approach to Modeling Weather and Climate. Journal of Climate 23(22):5933–5957, DOI 10.1175/2010JCLI3541.1, URL http://journals.ametsoc.org.ezproxy.lib.monash.edu.au/doi/abs/10.1175/2010JCLI3541.1

Martin GM, Bellouin N, Collins WJ, Culverwell ID, Halloran PR, Hardiman SC, Hinton TJ, Jones CD, McDonald RE, McLaren AJ, O'Connor FM, Roberts MJ, Rodriguez JM, Woodward S, Best MJ, Brooks ME, Brown AR, Butchart N, Dearden C, Derbyshire SH, Dharssi I, Doutriaux-Boucher M, Edwards JM, Falloon PD, Gedney N, Gray LJ, Hewitt HT, Hobson M, Huddleston MR, Hughes J, Ineson S, Ingram WJ, James PM, Johns TC, Johnson CE, Jones A, Jones CP, Joshi MM, Keen AB, Liddicoat S, Lock AP, Maidens AV, Manners JC, Milton SF, Rae JGL, Ridley JK, Sellar A, Senior CA, Totterdell IJ, Verhoef A, Vidale PL, Wiltshire A (2011) The HadGEM2 family of Met Office Unified Model Climate configurations. Geoscientific Model Development Discussions 4(2):765–841, DOI 10.5194/gmdd-4-765-2011, URL http://www.geosci-model-dev-discuss.net/4/765/2011/gmdd-4-765-2011.html

Rayner NA, Brohan P, Parker DE, Folland CK, Kennedy JJ, Vanicek M, Ansell TJ, Tett SFB (2006) Improved Analyses of Changes and Uncertainties in Sea Surface Temperature Measured In Situ since the Mid-Nineteenth Century: The HadSST2 Dataset. Journal of Climate 19(3):446–469, DOI 10.1175/JCLI3637.1, URL http://journals.ametsoc.org/doi/abs/10.1175/JCLI3637.1

Su H, Neelin J, Meyerson J (2005) Mechanisms for Lagged Atmospheric Response to ENSO SST Forcing*. Journal of climate 18(2002):4195–4215, URL http://journals.ametsoc.org/doi/abs/10.1175/JCLI3514.1

Sutton RT, Dong B, Gregory JM (2007) Land/sea warming ratio in response to climate change: IPCC AR4 model results and comparison with observations. Geophysical Research Letters 34(2):2–6, DOI 10.1029/2006GL028164, URL http://www.agu.org/pubs/crossref/2007/2006GL028164.shtml

Taylor KE, Stouffer RJ, Meehl GA (2012) An Overview of CMIP5 and the Experiment Design. Bulletin of the American Meteorological Society 93(4):485–498, DOI 10.1175/BAMS-D-11-00094.1, URL http://journals.ametsoc.org.ezproxy.lib.monash.edu.au/doi/abs/10.1175/BAMS-D-11-00094.1

Wang G, Dommenget D, Frauen C (Submitted) An evaluation of the CMIP3 and CMIP5 simulations in their skill of simulating the spatial structure of SST variability. Climate Dynamics

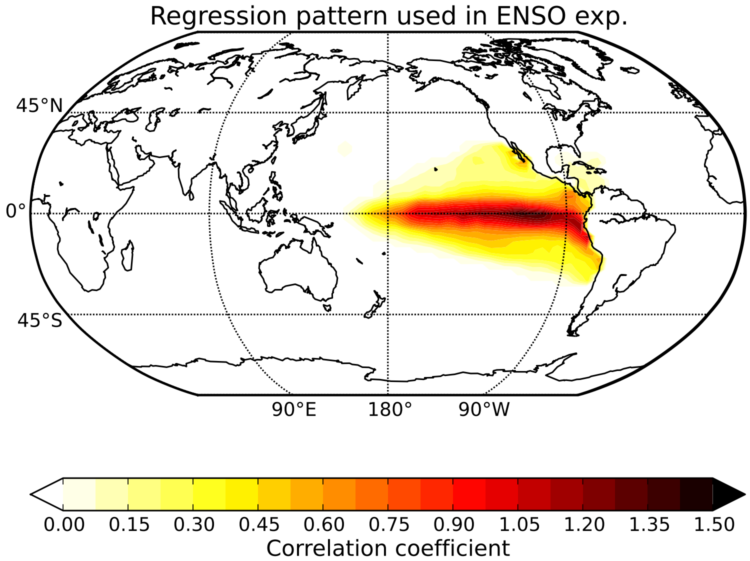

Fig. 1 Pattern used in ENSO experiments. Result of regression between NINO3 and global SST.

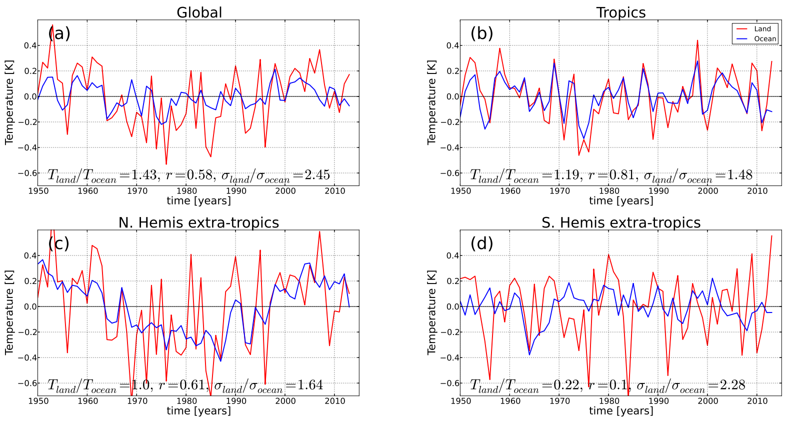

Fig. 2 Observational annual mean T_{land} and T_{ocean} using detrended HadSST2 and CruTEMP4 data

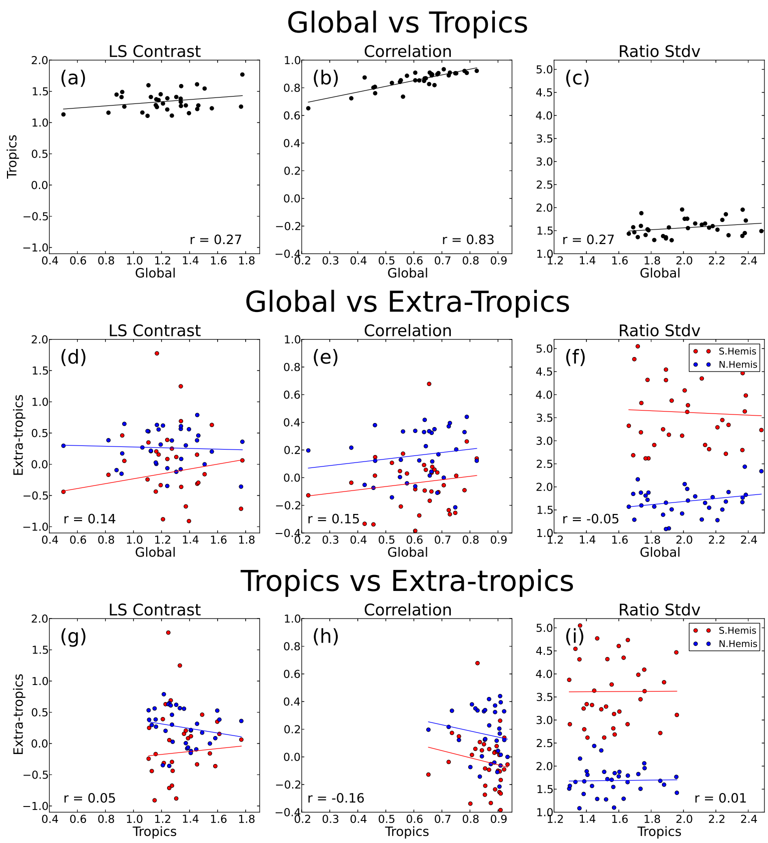

Fig. 3 Scatter plot with CMIP5 models showing relationship between global and tropical (top row) and global and extra-tropical (bottom row) values of the land/sea contrast (a,d), land/sea correlation (b,e) and ratio standard deviations (c,f).

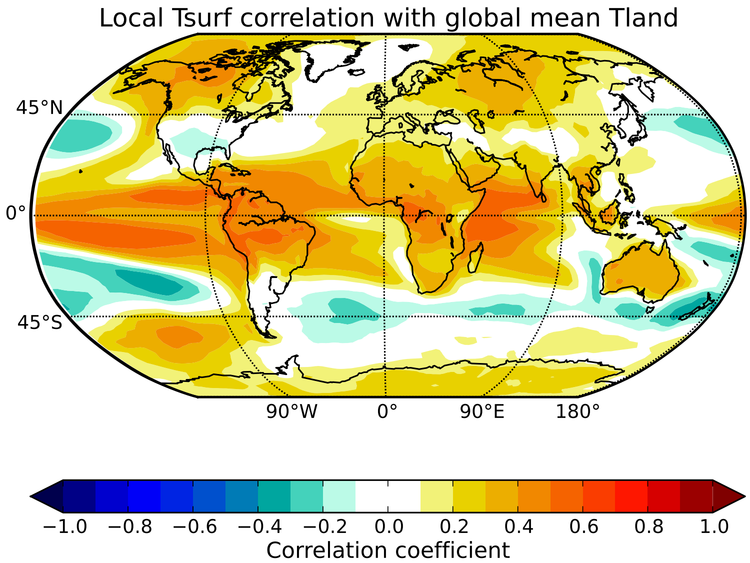

Fig. 4 Correlation between globally averaged T_{land} and T_{surf}, combined annual means from 35 CMIP5 pre-industrial control runs, 100 years from each model.

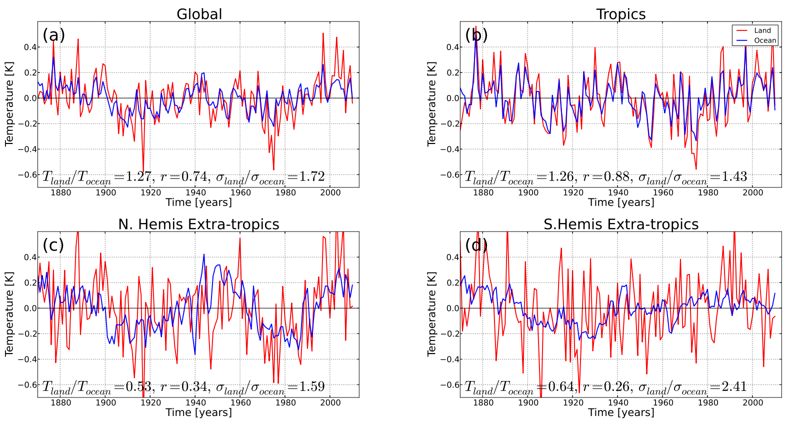

Fig. 5 Annual mean T_{land} and T_{ocean} for a) global b) tropical c) Northern Hemisphere extra-tropical d) Southern Hemisphere extra-tropical. AMIP run forced with detrended HadISST1.

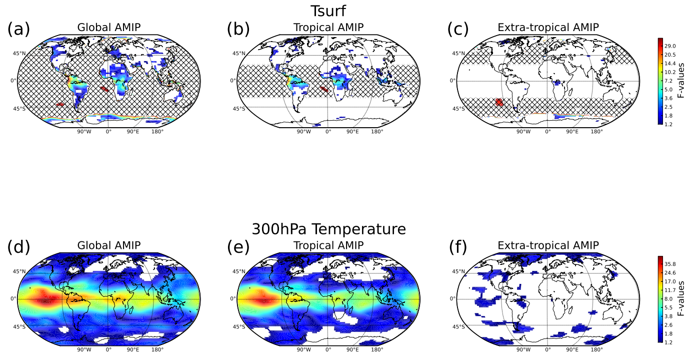

Fig. 6 F-test of annual mean temperature for AMIP-type runs. Surface temperature response on top row, 300hPa response on bottom row. a),d) AMIP run with detrended HadISST1 used globally b),e) AMIP-type run with detrended HadISST1 in extra-tropics, climatological SSTs elsewhere c),f) AMIP-type run with detrended HadISST1 in tropics, climatological SSTs elsewhere tropics. All values masked at 90% confidence levels. Hatching indicates areas of ocean with SST variability.

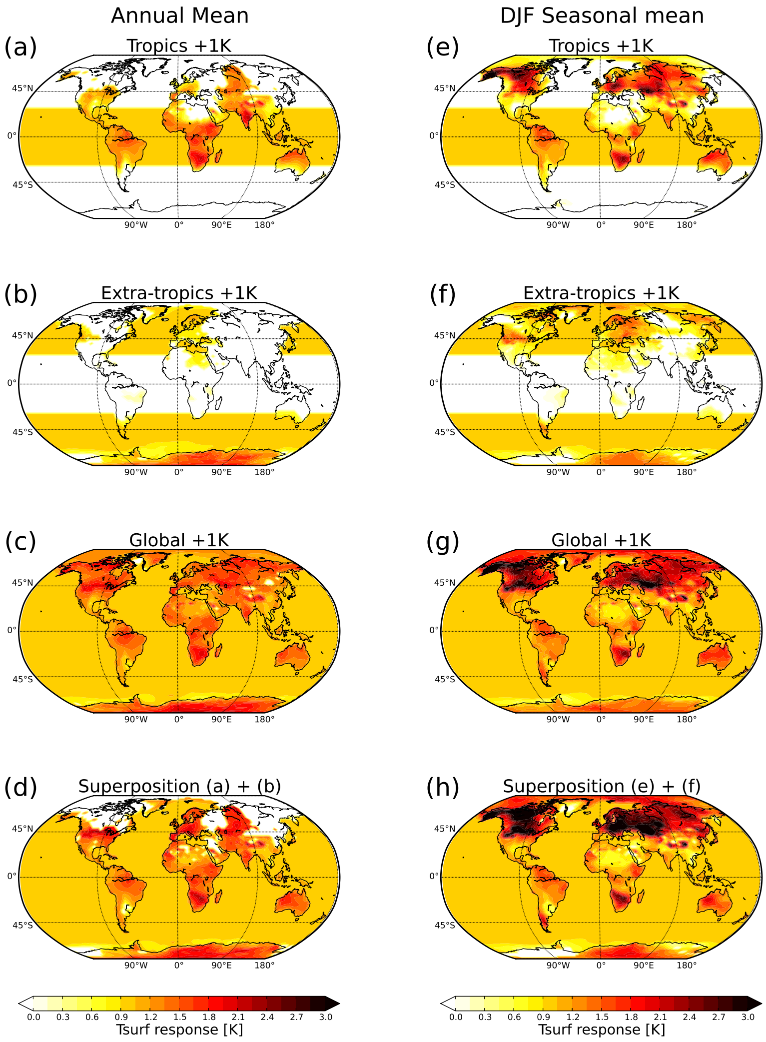

Fig. 7 Mean T_{surf} response for sensitivity experiments a) 1K added to tropical oceans b) 1K added to extra-tropical oceans c) 1K added to global oceans d) Combined response of tropical 1K oceans plus extra-tropical 1K ocean. Masked at 95% confidence levels.

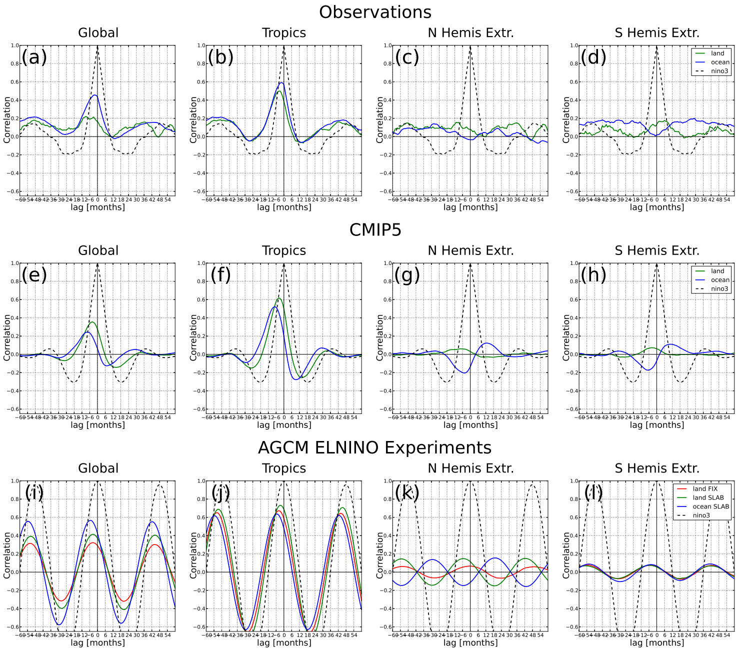

Fig. 8 Cross-correlations between the NINO3 region and land and ocean. Observations (top row), combined CMIP5 models (middle row), Two sensitivity experiments (bottom row); Atmospheric model forced with ENSO-like oscillation in tropical Pacific and fixed SSTs elsewhere (red line), slab ocean elsewhere (green, blue lines). Global land and ocean (a,e,i), tropical land and ocean (b,f,j), NH extra-tropical land and ocean (c,g,k) and SH extra-tropical land and ocean (d,h,l). NINO3 autocorrelation included for reference (black dashed line).

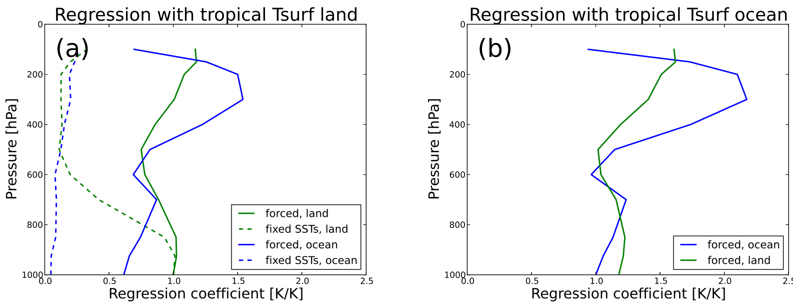

Fig. 9 Linear regression coefficients for temperature above tropical land and ocean as linear model of a) T_{land} (1000hPa surface) and b) T_{ocean}, for forced run (solid) and control run (dashed). i.e. $T_{plv,land} = aT_{sfc,land} + b$, and $T_{plv,ocean} = aT_{sfc,land} + b$

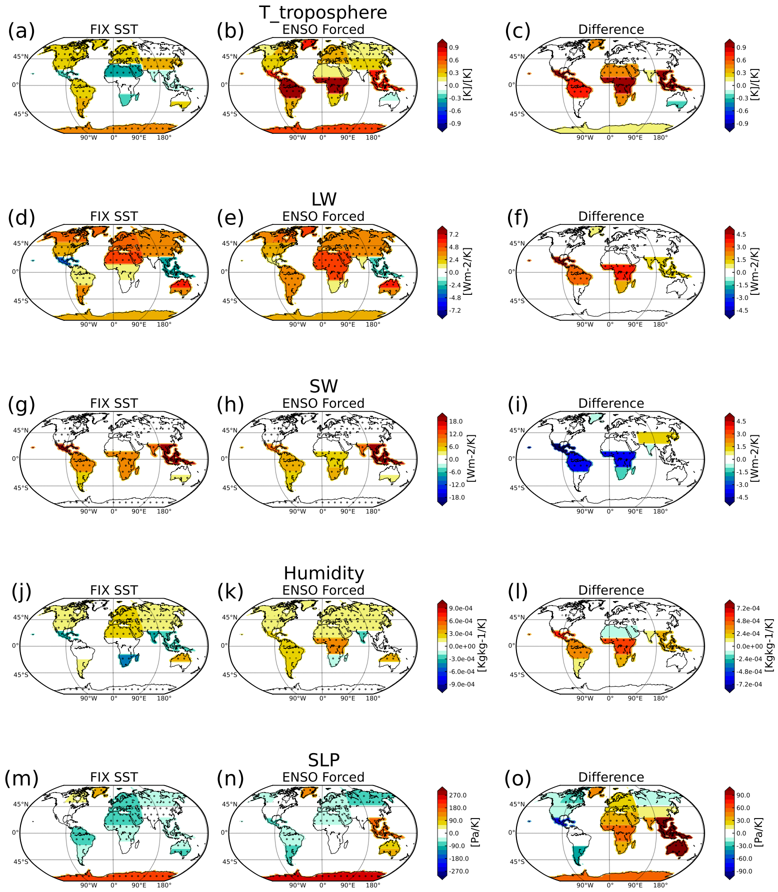

Fig. 10 Regression values between surface and variable averaged over regions. Control run (left), forced run (middle), difference (right). (a-c) Upper Tropospheric temperature (500-100hPa), (d-f) Downward longwave radiation, (g-i) Downward Shortwave radionation, (j-l) Specific Humidity 1.5m, (m-o) sea level pressure. Dotted regions indicate significance levels above 95%